ISCI, Volume *19*

Supplemental Information

Virus- and Interferon Alpha-Induced Transcriptomes of Cells from the Microbat *Myotis daubentonii*

Martin Hölzer, Andreas Schoen, Julia Wulle, Marcel A. Müller, Christian Drosten, Manja Marz, and Friedemann Weber

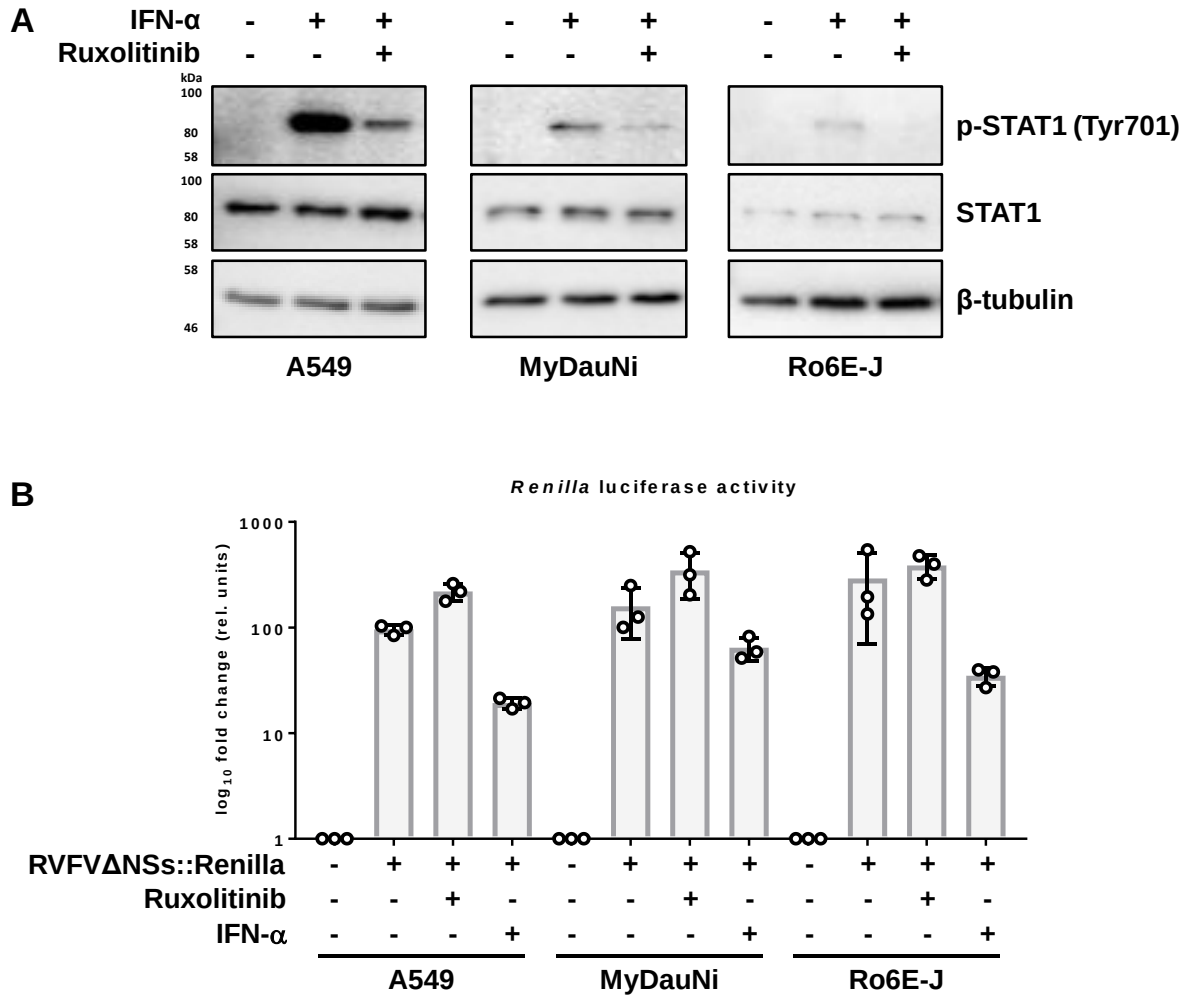

Figure S1, related to Figure 1. *Myotis daubentonii* kidney cell line MyDauNi/2c is fully IFN competent. (A) STAT1-dependent response to exogenous IFN. Human A549, *M. daubentonii* MyDauNi and *R. aegytiacus* Ro6E-J cells where treated with IFN-α, the JAK1/2 inhibitor Ruxolitinib, or were left untreated. Immunoblot analysis was performed with antibodies against the indicated antigens. Representative data from three independent experiments are shown. (B) Multiplication of an IFN-sensitive virus. Cells were pretreated with IFN or Ruxolitinib, infected with the IFN inducing and IFN-sensitive RVFVΔNSs::Renilla, and virus replication was measured by Renilla luciferase assays after 48 h of incubation. The graph shows the virus reporter activities normalized to uninfected background values for each cell line. Mean values and standard deviations from three independent replicates are shown.

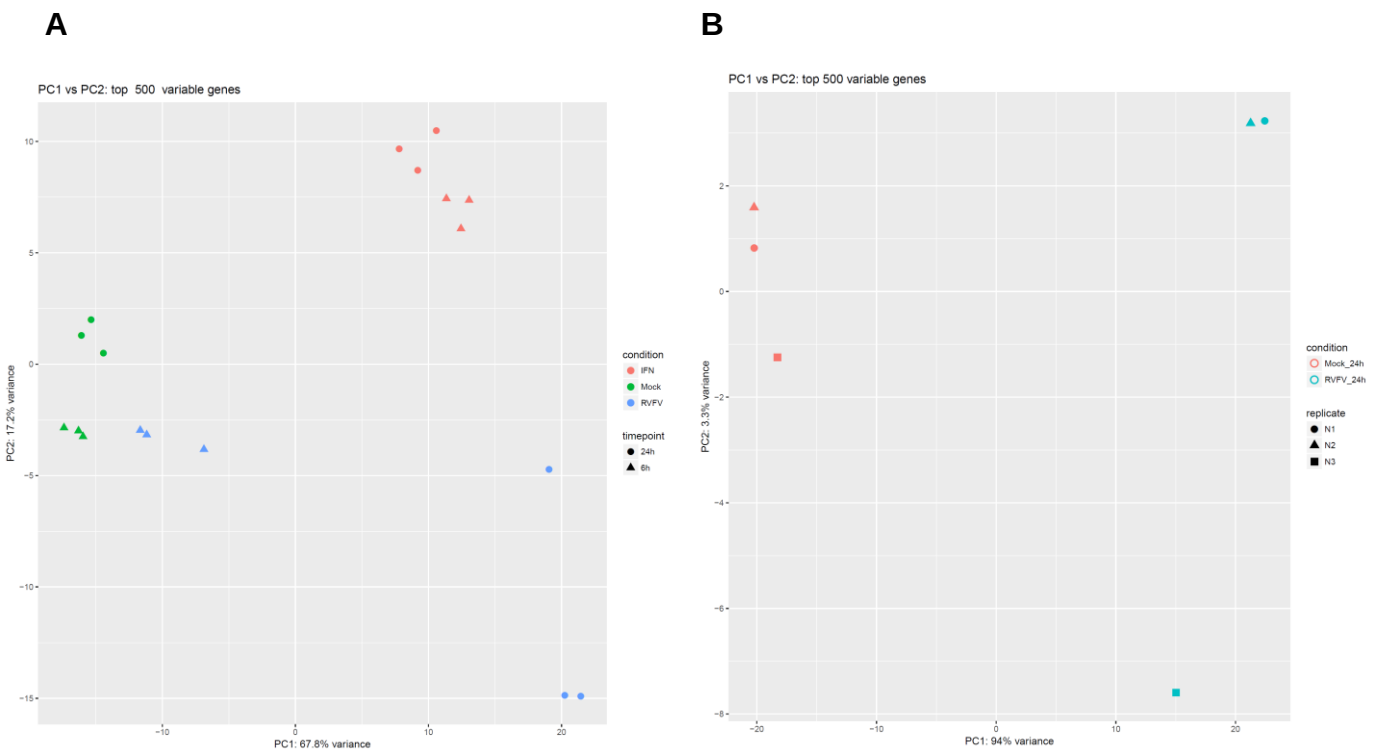

Figure S2, related to Figure 1. Principal component analysis. (A) PCA transformation based on the top 500 variant genes over all samples. One of the 24h RVFV mutant (Clone 13) samples seems to not cluster that well with the other replicates. (B) PCA transformation based on the top 500 variant genes between mock 24h and RVFV mutant 24h samples. The difference between the "outlier" virus-infected sample and the other two replicates accounts only for 3.3% (PC2) of the whole variation in the gene expression data.

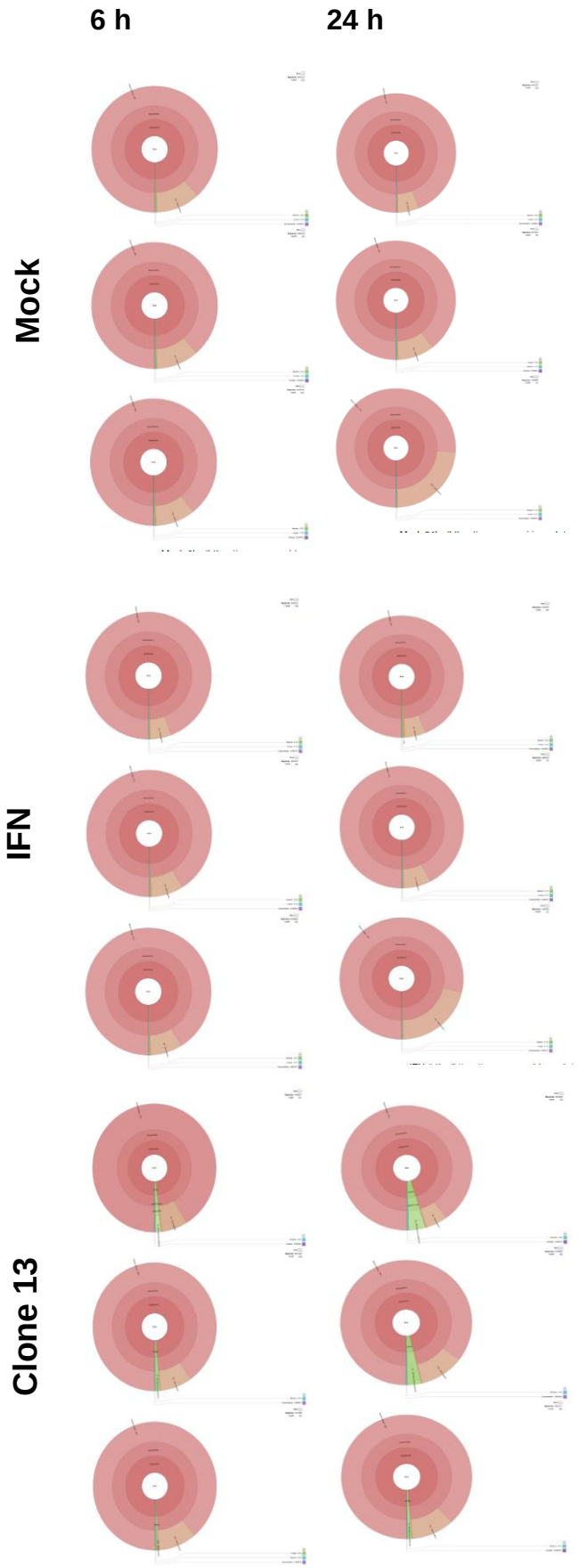

Figure S3, related to Figure 1. CLARK classification was run against NCBI RefSeq genomes of bacteria, viruses, fungi, human and a custom database comprising the *M. lucifugus* genome.

A

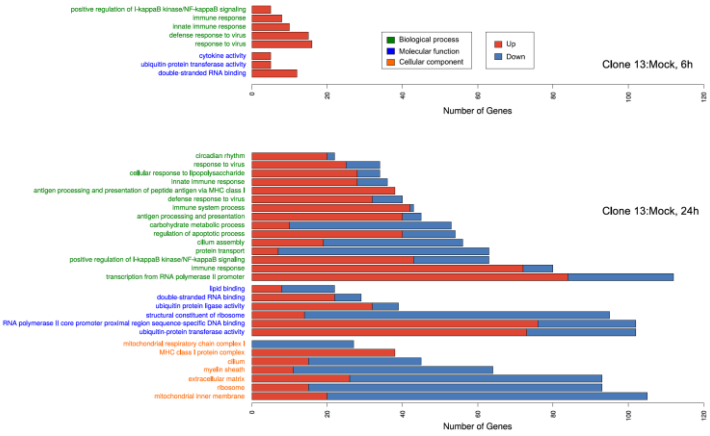

B

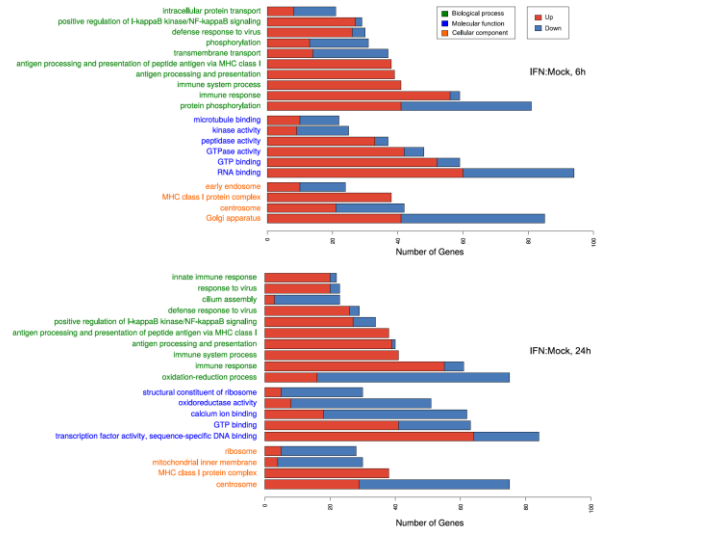

C

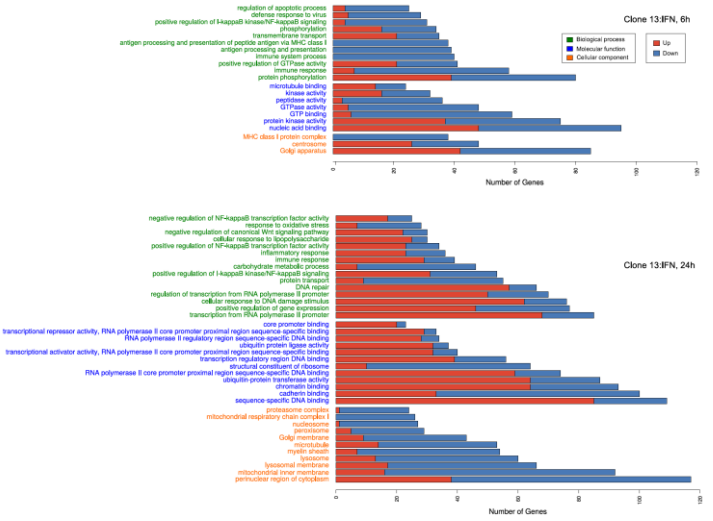

Figure S4, related to Figures 1, 2, 3, 4. Enriched GO terms based on pairwise comparisons. A: Mock vs. Clone13, B: Mock vs. IFN, C: IFN vs. Clone13.

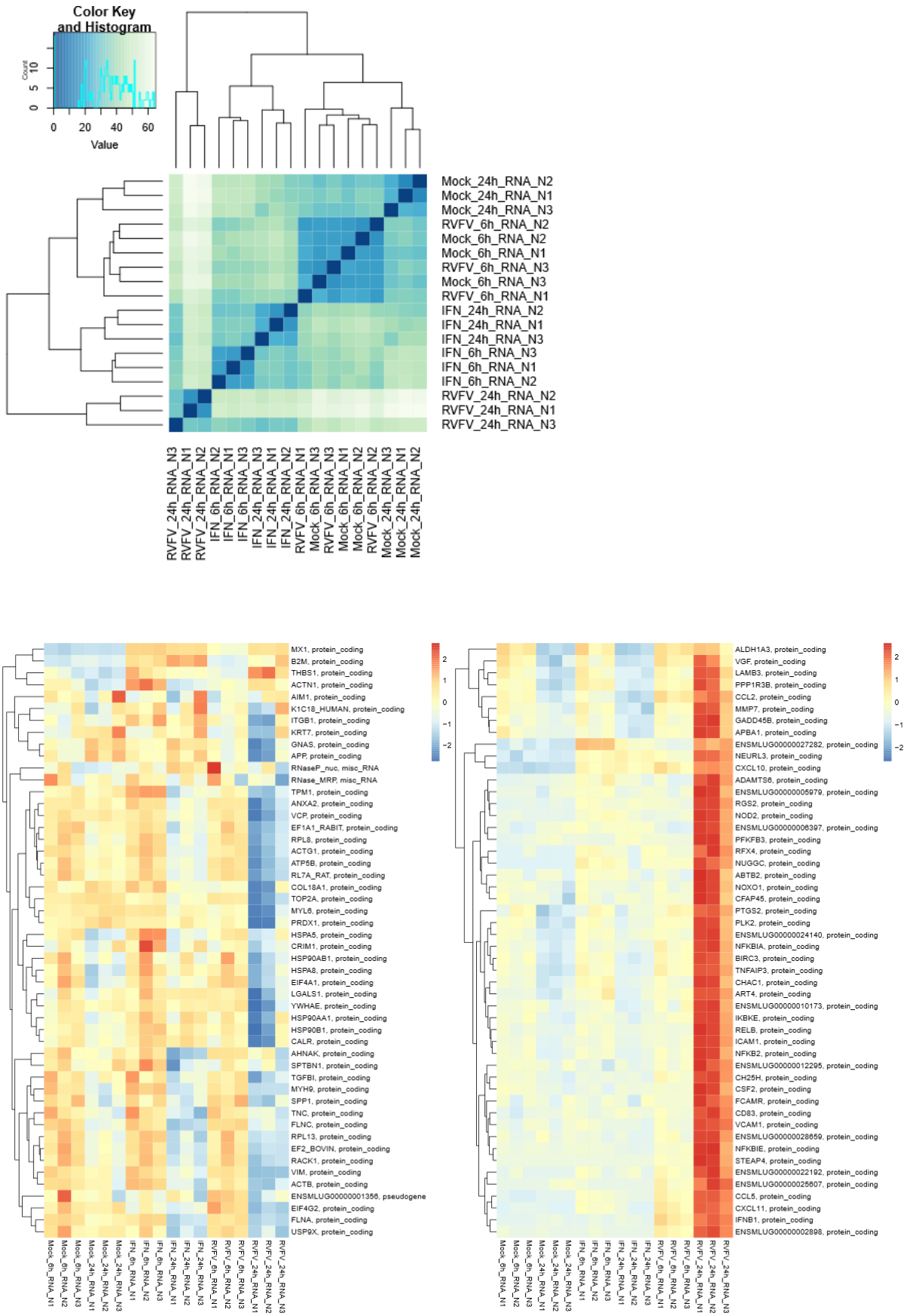

Figure S5, related to Figures 2, 3, and 4. DEG overview.

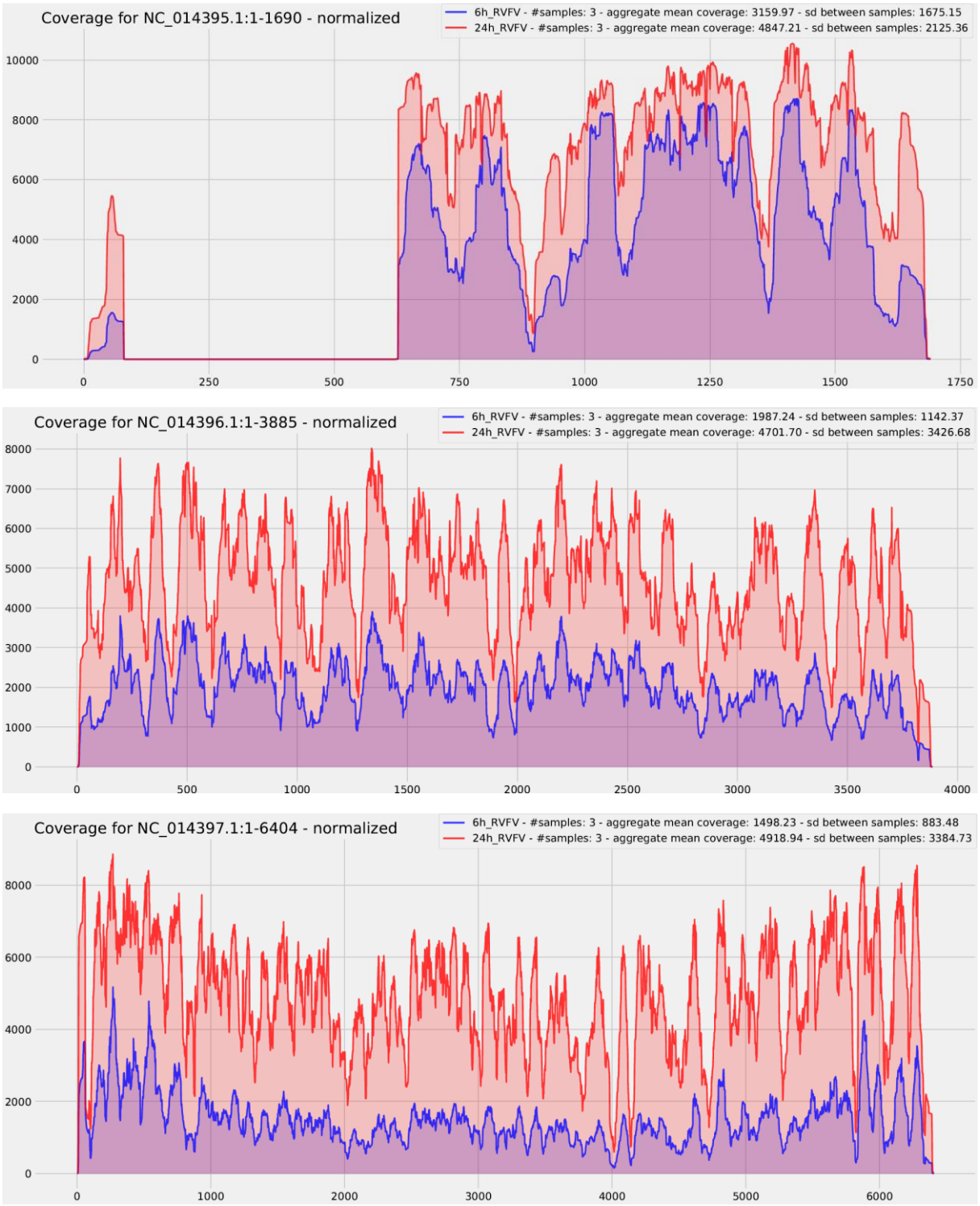

Figure S6, related to Figures 1, 2, 4. Coverage of the S, M, and L segment of the RVFV reference genome. Reference sequences for Clone 13 of the S, M, and L segment of RVFV were downloaded from the NCBI under RefSeq accessions Genbank: NC_014395.1 (S segment), Genbank: NC_014396.1 (M segment), Genbank: NC_014397.1 (L segment). The plots show the aggregate average coverage for the triplicates 6h and 24h post infection with the RVFV Clone13 mutant. Please note the Clone 13-specific deletion in the IFN antagonist NSs on the S segment that determines its high IFN induction capability.

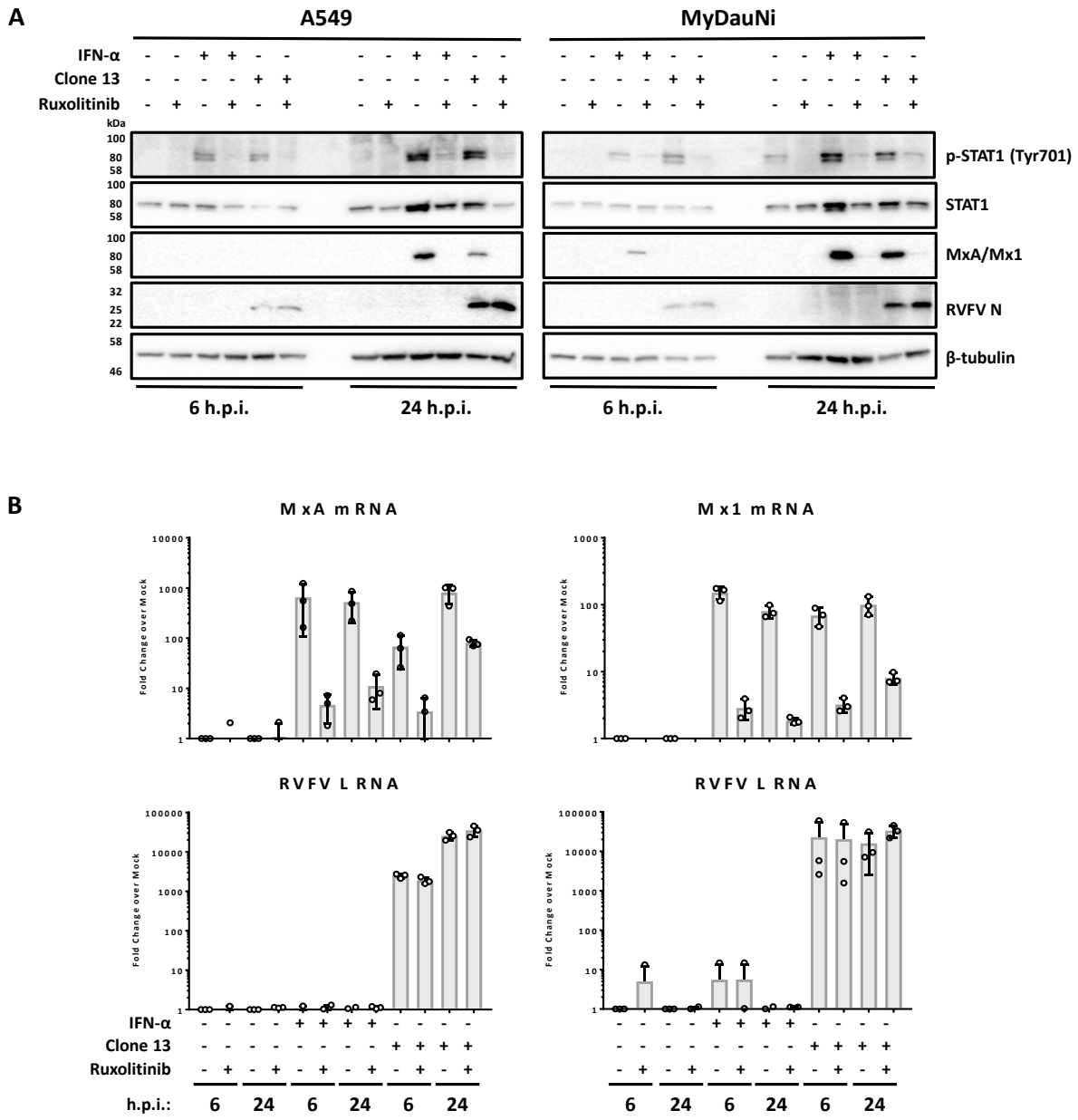

Figure S7, related to Figure 5. RT-qPCR confirmation of virus-only response genes - control experiments. Human A549 and *M. daubentonii* MyDauNi cells, treated or not with Ruxolitinib, were incubated with 1000 U/ml IFN-α or infected with Clone 13 (MOI 5) for 6 or 24 h, respectively. (A) Immunoblot analysis was performed with antibodies against the indicated antigens. Representative data from three independent experiments are shown. (B) RT-qPCR for MxA/Mx1 transcripts and the viral L segment, respectively. The graphs show the fold induction over mock, for the respective time point, with mean values and standard deviations from three independent replicates.

TRANSPARENT METHODS

KEY RESOURCES TABLE

REAGENT or RESOURCE	SOURCE	IDENTIFIER
Antibodies		
Rabbit polyclonal anti-phospho-Stat1 (Tyr701)	Cell Signaling	Cat# 9171
Mouse monoclonal anti-Stat1	BD Transduction Laboratories	Cat# 610185
Rabbit polyclonal anti- beta-tubulin	Abcam	Cat# ab6046
Mouse monoclonal anti-Mx (M143)	Georg Kochs, University of Freiburg, Germany	
Rabbit polyclonal anti-RVFV	Alejandro Brun, INIA, Madrid	
Virus Strains		
RVFVΔNSs::Renilla	Weber laboratory (Kuri et al., 2010)	N/A
Clone 13 (mutant RVFV strain)	Bouloy laboratory, Institute Pasteur, Paris (Billecocq et al., 2004)	N/A
Chemicals, Peptides, and Recombinant Proteins		
Pan-species IFN-α (B/D)	PBL Biomedical Laboratories	
Ruxolitinib	Selleckchem	Cat# S1378
Critical Commercial Assays		
Dual-Luciferase Reporter Assay System	Promega	Cat# E1960
RNeasy Plus Mini Kit (250)	Qiagen	Cat# 74106
PrimeScript RT Reagent Kit with gDNA Eraser	Takara	Cat# RR047A
SYBR Premix Ex Taq (Tli RNase H Plus) Kit	Takara	Cat# RR420
Premix Ex Taq (Probe qPCR) Kit	Takara	Cat# RR390
Experimental Models: Cell Lines		

A549 cells	Weber laboratory	N/A
MyDauNi/2c	Müller/Drosten laboratory	N/A
Ro6E-J cells cells	Müller/Drosten laboratory	N/A
Vero E6 cells	Weber laboratory	N/A
BHK cells	Weber laboratory	N/A
Oligonucleotides		
Human IFNB1	Qiagen	Cat# QT00203763
Human CCL4	Qiagen	Cat# QT01008070
Human CH25H	Qiagen	Cat# QT00202370
Human STEAP4	Qiagen	Cat# QT00081403
Human MxA	Qiagen	Cat# QT00090895
18S RNA	Qiagen	Cat# QT00199367
Primer for human IFNL2/3 RT-qPCR Forward: 5' GCCTCTGTCACCTTCAACCTC 3'	(Spann et al., 2004)	N/A
Primer for human IFNL2/3 RT-qPCR Reverse 5' GGAGGGTCAGACACACAGGT3'	(Spann et al., 2004)	N/A
Primer for *M. daubentonii* IFNB1 RT-qPCR Forward: 5' AAAGCAGCAATTCAGCCTGT 3'		
Primer for *M. daubentonii* IFNB1 RT-qPCR Reverse: 5' CTGCTGGAGCATCTCGTACA 3'		
Primer for *M. daubentonii* CCL4 RT-qPCR Forward: 5' TCTGCTCTCCAGTGCTCTCA 3'		
Primer for *M. daubentonii* CCL4 RT-qPCR Reverse: 5' AGATCTGTCTGCCCCTTTTG 3		
Primer for *M. daubentonii* IFNL3 RT-qPCR Forward: 5' CACATCCACTCCAAGCTTCA 3'		
Primer for *M. daubentonii* IFNL3 RT-qPCR Reverse: 5' TCAGCGACACATCTCAGGTC 3'		

Primer for *M. daubentonii* CH25H RT-qPCR Forward: 5' TCTTCCACACGCTCAACATC 3		
Primer for *M. daubentonii* CH25H RT-qPCR Reverse: 5' GGGGCGAAGTTGTAGTTGAA 3'		
Primer for *M. daubentonii* STEAP4 RT-qPCR Forward: 5' CCCAGAGTCCAATGCAGAGT 3'		
Primer for *M. daubentonii* STEAP4 RT-qPCR Reverse: 5' GTTGCAGGGGGTAGTTTTCA 3'		
Primer for *M. daubentonii* Mx1 RT-qPCR Forward: 5' CAGAGGGAGAGGGCTTTCTT 3		
Primer for *M. daubentonii* Mx1 RT-qPCR Reverse: 5' TCTGCTGGTTCTCCTTTATTTG 3'		
Primer for *M. daubentonii* 18S rRNA RT-qPCR Forward: 5' AAACGGCTACCACATCCAAG 3		
Primer for *M. daubentonii* 18S rRNA RT-qPCR Reverse: 5' CCTCCAATGGATCCTCGTTA 3'		
Primer for RVFV L segment RNA RT-qPCR	(Bird et al., 2007)	
Software and Algorithms		
Ensembl (Myoluc2.0, release 86)		
GraphPad Prism 7		
STAR (v2.5.2)	(Dobin and Gingeras, 2015)	
CLARK (v1.2.5)	(Ounit et al., 2015)	
Krona (v2.7)	(Ondov et al., 2011)	
blastx (v2.4.0+)		
Trinotate pipeline (v3.0.2)	https://trinotate.github.io/	
featureCounts(v1.5.0)	(Liao et al., 2014)	
ReportingTools package	(Huntley et al., 2013)	
Piano package	(Varemo et al., 2013)	

PCAGO web service	https://doi.org/10.1101/433078	
BinPacker (v1.1)	(Liu et al., 2016)	
IDBA-Tran (v1.1.1)	(Peng et al., 2013)	
SPAdes in single-cell and RNA modus (v3.10.1)	(Bankevich et al., 2012)	
SOAPdenovo-trans (v1.03)	(Xie et al., 2014)	
Trinity (v2.3.2)	(Grabherr et al., 2011)	
CD-HIT-EST (v4.6; -c 0.95)	(Fu et al., 2012)	
MAFFT (v7.402; L-INS-i parameter)	(Katoh and Standley, 2013)	
RAxML (v8.0.25)	(Stamatakis, 2014)	
Newick Utilities suite (v1.6)	(Junier and Zdobnov, 2010)	
Inkscape (v0.92.1)	https://inkscape.org	

CONTACT FOR REAGENT AND RESOURCE SHARING

Further information and requests for resources and reagents should be directed to and will be fulfilled by the Lead Contact, Friedemann Weber (friedemann.weber@vetmed.uni-giessen.de).

EXPERIMENTAL MODELS AND SUBJECT DETAILS

Cells, viruses, and reagents

Human lung A549 and the *M. daubentonii* kidney cell line MyDauNi/2c (Fuchs et al., 2017; Muller et al., 2012) were propagated in CCM-34 medium (4,5 g/L DMEM supplemented with 200 µM L-Alanine, 225 µM L-Aspartic acid, 933 µM Glycin, 510 µM L-Glutamic acid, 217 µM L-Proline, 184 µM Hypoxanthine, 0,1 mg/L Biotin, 44 mM NaHCO3, 10 % FBS, 10 U/L Penicillin, 10 µg/L Streptomycin and 292 µg/L L-glutamine. *R. aegytiacus* Ro6E-J cells (Jordan et al., 2009), human A549 cells, simian VeroE6 cells and hamster BHK cells were propagated in DMEM (Gibco/ Thermo Fisher Scientific) supplemented with 100 µM Glycine, 100 µM L-Alanine, 100 µM L-Asparagine, 100 µM L-Aspartic acid, 100 µM L-Glutamic Acid, 100 µM L-Proline, 100 µM L-Serine, 10 % FBS, 10 U/L Penicillin, 10 µg/L Streptomycin and 292 µg/L L-Glutamine. Recombinant Rift Valley fever virus mutant (RVFVΔNSs::Renilla)(Kuri et al., 2010) and the natural NSs-deficient mutant Clone 13 (Billecocq et al., 2004), were propagated on BHK cells and titrated on Vero E6 cells as described.

Assays for cellular IFN competence

To test for STAT1-dependent responses, cells where either treated with 1 µM of Ruxolitinib for 1 h, and/or 500 U/ml pan-species IFN-α (B/D) for 30 min, or left untreated. After lysis of cells, immunoblot analysis was performed with primary antibodies against phospho-Stat1, Stat1 (both 1:1000), and tubulin (1:2000).

To test for the ability to produce antiviral IFN in response to infection, cells were pretreated with 30 nM Ruxolitinib (1 h prior to infection) or 500 U/ml IFN-α (B/D) (16 h prior to infection), or left untreated. The cells were then infected with RVFVΔNSs::Renilla at a multiplicity of infection (MOI) of 1. Ruxolitinib and IFN were added also to the cell culture medium for the duration of the infection. At 48 h post-infection, cells were lysed and subjected to Renilla luciferase assays as described by the manufacturer (Promega Dual Luciferase kit) on a TriStar2 Multimode Reader LB 942 (Berthold).

Next-Generation Sequencing design and RNA-Seq

Total cellular RNA was isolated at 6 h and at 24 h post infection (1.200.000 cells per condition and time point), approved for their integrity using an Agilent 2100 Bioanalyzer, and subjected to RNA deep sequencing. For each total RNA sample cDNA libraries were prepared utilizing the Illumina Ribo-Zero rRNA Removal Kit for human/mouse/rat (hereafter rRNA-). Importantly, no polyA selection was applied. Overall, 18 rRNA- libraries were sequenced on six HiSeq 2500 lanes with 51 cycles resulting in 60-70 million strand-specific single-end reads per sample (Tab. S1). The complete experiment was performed in three independent, biological replicates. The raw read data was deposited in the GEO database under accession number GEO: GSE121301.

Data processing, quality control and mapping

Since no reference genome for *M. daubentonii* is publicly available, we downloaded the reference sequence and annotation of the closely related *M. lucifugus* from Ensembl (Myoluc2.0, release 86). Reference sequences for the L, M, and S segment of RVFV were downloaded from the NCBI under RefSeq accessions NC014397.1, NC014395.1, and NC014396.1. The genomic sequence of *M. lucifugus* and the RVFV sequences were concatenated for mapping the RNA-Seq-derived short reads. Prior to mapping, all samples were quality checked with FastQC and quality trimmed with a Q20 threshold and a window size of length 4 using Prinseq (v0.20.3) (Schmieder and Edwards, 2011). Reads shorter than 15 nt were discarded from the analysis. We used SortMeRNA (v2.1) (Kopylova et al., 2012) to detect and remove ribosomal RNAs, possibly still remaining after the ribosomal depletion step during cDNA library preparation. The quality-controlled and rRNA-depleted reads were mapped to the concatenated reference genomes of *M. lucifugus* and RVFV using STAR (v2.5.2) (Dobin and Gingeras, 2015) with an adjusted --outFilterScoreMinOverLread and --outFilterMatchNminOverLread of 0.4.

Read classification and Krona visualization

To check for possible contaminations in the RNA and the amount of viral reads in each sample, we used CLARK (v1.2.5) (Ounit et al., 2015) to classify the quality-checked reads against the NCBI RefSeq databases for viruses, bacteria, fungi, and human. We added the Ensembl *M. lucifugus* genome as a custom database and visualized the classification results of each sample with Krona (v2.7) (Ondov et al., 2011).

Extension of the *M. lucifugus* annotation

We used blastx (v2.4.0+) against the Uniprot/SwissProt database created with the Trinotate pipeline (v3.0.2; https://trinotate.github.io/) to extend the Ensembl gene annotation of *M. lucifugus*. All blast hits that were considered as true positive hits had to meet an E-value threshold of 10^{-4}, a sequence identity of at least 50% and an alignment length of at least 50%. If multiple hits for one sequence passed our filter settings, we selected the one with the best E-value. Based on this approach, we were able to assign a gene name and function to additional 4,844 sequences out of 7,101 CDS without a functional description in the Ensembl annotation for *M. lucifugus*. Additional homologous gene annotations were marked with a _<SPECIES> tag in the electronic supplement to distinguish between the original Ensembl annotation and our extension.

Based on our strand-specific RNA-Seq data and with the help of our *de novo* assembly, we found various IFN genes to be annotated on the wrong strand in the Ensembl annotation of *M. lucifugus*. Therefore, these genes got initially zero read counts when estimating expression values with featureCounts (v1.5.0) (Liao et al., 2014). To also take these genes into consideration, we adjusted the Ensembl annotation and changed the strand from '+' to '-' for the following gene IDs: ENSMLUG00000026947 (IFNA5_HUMAN), ENSMLUG00000027734, ENSMLUG00000023736 (IFNW2_HORSE), ENSMLUG00000027612, ENSMLUG00000028931 (IFNW2_HORSE), ENSMLUG00000024850, ENSMLUG00000027376. Moreover, IRF7 was before not annotated at all in the *M. lucifugus* genome and had to be manually corrected. We calculated the position of IRF7 in the *M. lucifugus* genome based on our mapped reads and NCBI blast searches to finally add its annotation on contig

AAPE02063415:16558-16759 on the minus strand. In addition, we identified ENSMLUG00000025338 as being ISG15.

RNA quantification, normalization and differential gene expression

We used featureCounts to quantify the mapped reads based on our extended and corrected Ensembl annotation (originally release 86) of *M. lucifugus* comprising 25,849 genes (19,728 coding for proteins). Reads were counted strand-specific on exon level and accumulated per gene ID to obtain one count per gene. Only uniquely mapped reads were used in the differential gene expression analysis and further evaluations.

The read counts were passed to DESeq2 (v1.16.1) (Love et al., 2014) to call significantly (adjusted $p \leq 0.05$) differentially expressed genes and to calculate fold changes between the different time points and conditions. To reduce the amount of low expressed genes and false positive hits, the DESeq2 results were additionally filtered by calculating TPM (transcripts per million) values for each gene and each sample as:

$$TPM_i = \frac{c_i}{l_i} \times \left(\frac{1}{\sum_{j \in N} \frac{c_j}{l_j}} \right) \times 10^6$$

where c_i is the raw read count of gene i, l_i is the cumulative exon length of gene i and N is the number of all genes in the given annotation. For each gene, we calculated six mean TPM values (TPM_M), based on the three biological replicates corresponding to the mock, IFN and Clone 13-infected samples at the two time points. If a protein-coding gene showed a $TPM_M > 1$ in at least one of the six conditions, it was considered as expressed and used for further analyses. Genes that did not show a $TPM_M > 1$ in at least one condition were marked and discarded from further analyses.

We used various R packages for visualization and data assessment, comprising extended functionalities of the DESeq2 package such as principal component analyses, gene expression scatter plots and heat maps. We used the ReportingTools package (Huntley et al., 2013) to generate interactive web pages of significantly differential expressed genes and to build expression box plots for all genes and samples. GO term enrichment and visualization of the most significant regulated gene sets was performed with the Piano package (Varemo et al., 2013).

Principal component analyses were performed using the PCAGO web service (https://doi.org/10.1101/433078). As input, unique read counts of all 18 samples were used and DESeq2-normalized and rlog-transformed with the build in functionalities of the web service. Genes with zero or constant read counts were removed prior PCA and the top 500 variant genes were finally used for the transformation shown in Fig.3. Supplemental 2d- and 3d-PCA movies were generated starting with the top 10 variant genes and adding step-wise 10 genes until reaching all 21,791 genes without zero or constant read count.

De novo transcriptome assembly

Based on a comparison of current *de novo* assembly tools for short-read RNA-Seq data (Holzer and Marz, 2019), we used SPAdes in single-cell and RNA modus (v3.10.1) (Bankevich et al., 2012), SOAPdenovo-trans (v1.03) (Xie et al., 2014), and Trinity (v2.3.2) (Grabherr et al., 2011) to build a comprehensive transcriptome assembly for *M. daubentonii*. As input, the quality-checked reads of all 18 samples were used. All assembly tools were executed with default parameters and, if possible, in strand-specific mode. The resulting contigs of all tools were merged with CD-HIT-EST (v4.6; -c 0.95) (Fu et al., 2012) and the final assembly was used for homology searches and to confirm observations obtained from the *M. lucifugus*-based genome analyses. To investigate also (*de novo*) transcripts and isoforms differing between the conditions, triplicate samples were merged and assembled with Trinity only.

Phylogenetic analysis of BST2

We downloaded twelve CDS of mammalian BST2 genes for *Pteropus vampyrus* (ENSPVAG00000007879), *Rousettus aegyptiacus* (NW_015494646), *Sus scrofa* (ENSSSCG00000033453), *Rattus norvegicus* (ENSRNOG00000059900), *Ovis aries* (ENSOARG00000025182, ENSOARG00000016787), *Gorilla gorilla* (ENSGGOG00000015278), *Canis familiaris* (ENSCAFG00000031353), *Bos taurus* (ENSBTAG00000008021), *Homo sapiens* (ENSG00000130303), *Mus musculus* (ENSMUSG00000046718), and *Pan troglodytes* (ENSPTRG00000010672) from Ensembl (release 93) and NCBI. We expanded this list by four potential BST2 paralogous genes, identified with the help of our extended annotation, from the *M. lucifugus* genome: ENSMLUG00000023562, ENSMLUG00000023691, ENSMLUG00000026989, and ENSMLUG00000029243. Furthermore, we extracted three potential BST2 transcripts from the *de novo* transcriptome assembly of *M. daubentonii*. Interestingly, we were only able to identify three BST2-like transcripts with a differing sequence in the assembly. Overall, we aligned 18 BST2-coding sequences with MAFFT (Katoh and Standley, 2013) (v7.402; L-INS-i parameter) and calculated a phylogenetic tree with RAxML (v8.0.25) (Stamatakis, 2014) using 1000 bootstraps, the GTRGAMMA model, and the primate BST2 CDS as outgroups. We used Inkscape (v0.92.1; available from https://inkscape.org) to finalize the tree and other figures for publication.

Verification of uniquely virus-regulated genes

A549 cells and MyDauNi cells (5×10E4 per well) where seeded in 24-well plates, grown overnight, and then either infected with RVFV Clone 13 (MOI 5), incubated with 1000 U/ml IFN-α (B/D), or left untreated, all with or without 1 µM Ruxolitinib as indicated. Cells were kept under the respective conditions and total RNA isolated 6 and 24 h post-infection using the RNeasy Mini Kit (Qiagen). A total of 100 ng RNA/sample was used for cDNA synthesis using the PrimeScript RT Reagent Kit with gDNA Eraser (Takara) according to manufacturer's instructions. The kit included a step for removal of possible contamination by genomic DNA. RT-qPCR was performed using the SYBR Premix Ex Taq (Tli RNase H Plus) and the Premix Ex Taq (Probe qPCR) Kit (Takara) on a StepOnePlus Real-Time PCR machine (Applied Biosystems). For primer sequences, see Key Resources Table. All data obtained were normalised against the 18S RNA signal using the ddCT method.

To confirm IFN competence and Ruxolitinib efficacy, cells infected and treated as indicated above were analysed by immunoblot with primary antibodies against phospho-Stat1, Stat1 and tubulin as indicated, and against Mx1 and RVFV N at 1:1000 and 1:2000, respectively.

Electronic Supplement

The electronic supplement can be found at https://www.rna.uni-jena.de/supplements/mda/ comprising additional information about the RNA-Seq quality and read pre-processing, mapping statistics, PCA plots and videos, a read classification with Clark, GO term enrichment, full tables (including Excel) and further statistics for all differential expressed genes of each pairwise comparison, and coverage plots of the viral reads mapping to the S, L, and M segment of the RVFV reference genome. We used the DESeq2 results and the visualizations of the ReportingTools (Huntley et al., 2013) package to build an interactive gene observer (IGO), containing 1,448 genes that have a significant hit (q-value < 0.05) and an absolute fold change > 1 in at least one of the four comparisons Mock:IFN 6 h, Mock:IFN 24 h, Mock:Clone13 6 h, and Mock:Clone13 24 h. Our online tool is available at https://www.rna.uni-jena.de/supplements/mda/report.html and can be easily used to search for gene names and Ensembl gene IDs of the *M. lucifugus* reference genome used.

For full reproducibility of our study, we also uploaded the raw read data in the GEO database under accession number GEO: GSE121301. Moreover, all intermediate files such as the quality-trimmed and rRNA-cleaned reads of all 18 samples, mappings, the extended genome annotation and raw read counts to the Open Science Framework under https://doi.org/10.17605/OSF.IO/X9KAD.

REFERENCES

Bankevich, A., Nurk, S., Antipov, D., Gurevich, A.A., Dvorkin, M., Kulikov, A.S., Lesin, V.M., Nikolenko, S.I., Pham, S., Prjibelski, A.D*., et al.* (2012). SPAdes: a new genome assembly algorithm and its applications to single-cell sequencing. J Comput Biol *19*, 455-477.

Billecocq, A., Spiegel, M., Vialat, P., Kohl, A., Weber, F., Bouloy, M., and Haller, O. (2004). NSs protein of Rift Valley fever virus blocks interferon production by inhibiting host gene transcription. Journal of virology *78*, 9798-9806.

Bird, B.H., Bawiec, D.A., Ksiazek, T.G., Shoemaker, T.R., and Nichol, S.T. (2007). Highly sensitive and broadly reactive quantitative reverse transcription-PCR assay for high-throughput detection of Rift Valley fever virus. J Clin Microbiol *45*, 3506-3513.

Dobin, A., and Gingeras, T.R. (2015). Mapping RNA-seq Reads with STAR. Curr Protoc Bioinformatics *51*, 11 14 11-19.

Fu, L., Niu, B., Zhu, Z., Wu, S., and Li, W. (2012). CD-HIT: accelerated for clustering the next-generation sequencing data. Bioinformatics *28*, 3150-3152.

Fuchs, J., Holzer, M., Schilling, M., Patzina, C., Schoen, A., Hoenen, T., Zimmer, G., Marz, M., Weber, F., Muller, M.A*., et al.* (2017). Evolution and Antiviral Specificities of Interferon-Induced Mx Proteins of Bats against Ebola, Influenza, and Other RNA Viruses. Journal of virology *91*.

Grabherr, M.G., Haas, B.J., Yassour, M., Levin, J.Z., Thompson, D.A., Amit, I., Adiconis, X., Fan, L., Raychowdhury, R., Zeng, Q.D*., et al.* (2011). Full-length transcriptome assembly from RNA-Seq data without a reference genome. Nat Biotechnol *29*, 644-U130.

Holzer, M., and Marz, M. (2019). De novo transcriptome assembly: A comprehensive cross-species comparison of short-read RNA-Seq assemblers. Gigascience *8*.

Huntley, M.A., Larson, J.L., Chaivorapol, C., Becker, G., Lawrence, M., Hackney, J.A., and Kaminker, J.S. (2013). ReportingTools: an automated result processing and presentation toolkit for high-throughput genomic analyses. Bioinformatics *29*, 3220-3221.

Jordan, I., Horn, D., Oehmke, S., Leendertz, F.H., and Sandig, V. (2009). Cell lines from the Egyptian fruit bat are permissive for modified vaccinia Ankara. Virus research *145*, 54-62.

Junier, T., and Zdobnov, E.M. (2010). The Newick utilities: high-throughput phylogenetic tree processing in the UNIX shell. Bioinformatics *26*, 1669-1670.

Katoh, K., and Standley, D.M. (2013). MAFFT multiple sequence alignment software version 7: improvements in performance and usability. Mol Biol Evol *30*, 772-780.

Kopylova, E., Noe, L., and Touzet, H. (2012). SortMeRNA: fast and accurate filtering of ribosomal RNAs in metatranscriptomic data. Bioinformatics *28*, 3211-3217.

Kuri, T., Habjan, M., Penski, N., and Weber, F. (2010). Species-independent bioassay for sensitive quantification of antiviral type I interferons. Virology journal *7*, 50.

Liao, Y., Smyth, G.K., and Shi, W. (2014). featureCounts: an efficient general purpose program for assigning sequence reads to genomic features. Bioinformatics *30*, 923-930.

Liu, J., Li, G., Chang, Z., Yu, T., Liu, B., McMullen, R., Chen, P., and Huang, X. (2016). BinPacker: Packing-Based De Novo Transcriptome Assembly from RNA-seq Data. PLoS Comput Biol *12*, e1004772.

Love, M.I., Huber, W., and Anders, S. (2014). Moderated estimation of fold change and dispersion for RNA-seq data with DESeq2. Genome biology *15*, 550.

Muller, M.A., Raj, V.S., Muth, D., Meyer, B., Kallies, S., Smits, S.L., Wollny, R., Bestebroer, T.M., Specht, S., Suliman, T*., et al.* (2012). Human Coronavirus EMC Does Not Require the SARS-Coronavirus Receptor and Maintains Broad Replicative Capability in Mammalian Cell Lines. Mbio *3*.

Ondov, B.D., Bergman, N.H., and Phillippy, A.M. (2011). Interactive metagenomic visualization in a Web browser. BMC Bioinformatics *12*, 385.

Ounit, R., Wanamaker, S., Close, T.J., and Lonardi, S. (2015). CLARK: fast and accurate classification of metagenomic and genomic sequences using discriminative k-mers. BMC genomics *16*.

Peng, Y., Leung, H.C., Yiu, S.M., Lv, M.J., Zhu, X.G., and Chin, F.Y. (2013). IDBA-tran: a more robust de novo de Bruijn graph assembler for transcriptomes with uneven expression levels. Bioinformatics *29*, i326-334.
Schmieder, R., and Edwards, R. (2011). Quality control and preprocessing of metagenomic datasets. Bioinformatics *27*, 863-864.
Spann, K.M., Tran, K.C., Chi, B., Rabin, R.L., and Collins, P.L. (2004). Suppression of the induction of alpha, beta, and gamma interferons by the NS1 and NS2 proteins of human respiratory syncytial virus in human epithelial cells and macrophages. Journal of virology *78*, 4363-4369.
Stamatakis, A. (2014). RAxML version 8: a tool for phylogenetic analysis and post-analysis of large phylogenies. Bioinformatics *30*, 1312-1313.
Varemo, L., Nielsen, J., and Nookaew, I. (2013). Enriching the gene set analysis of genome-wide data by incorporating directionality of gene expression and combining statistical hypotheses and methods. Nucleic acids research *41*, 4378-4391.
Xie, Y., Wu, G., Tang, J., Luo, R., Patterson, J., Liu, S., Huang, W., He, G., Gu, S., Li, S.*, et al.* (2014). SOAPdenovo-Trans: de novo transcriptome assembly with short RNA-Seq reads. Bioinformatics *30*, 1660-1666.